*Anal. Bioanal. Electrochem.*, Vol. 11, No. 12, 2019, 1747-1769
Archive of SID

**Analytical & Bioanalytical Electrochemistry**

2019 by CEE
www.abechem.com

*Review*

# The Influence of Grain Refinement on the Semiconducting Properties of Passive Films Formed on Ferritic Stainless Steels: A Review

**Arash Fattah-alhosseini* and Kazem Babaei**

*Department of Materials Engineering, Bu-Ali Sina University, Hamedan 65178-38695, Iran*

*Corresponding Author, Tel.: +988138292505; Fax: +988138257400

E-Mail: a.fattah@basu.ac.ir

*Received: 28 October 2019 / Accepted with minor revision: 9 November 2019 / Published online: 31 December 2019*

**Abstract**- Ferritic stainless steels are cheaper than austenitic stainless steels and if their behavior could be improved, both electrochemically and mechanically, they are able to rival and be substituted by a few austenitic grades in some specific usages. Numerous approaches have been utilized to produce the bulk fine-grained (FG) stainless steels so far. There are just two mechanical methods to get FG structures: procedures of advanced thermomechanical and severe plastic deformation techniques. The literature review clearly reveals the semiconducting properties of ferritic stainless steel (especially FG structures) that have been rarely investigated. So, the first aim of this paper is to review the semiconducting behaviors of the passive layers being formed on this type of stainless steels. In the following, we study influence of grain refinement on the semiconducting properties of produced passive films on FG ferritic stainless steels have been evaluated using Mott–Schottky analysis.

**Keywords-** Ferritic stainless steel, Grain refinement, Semiconducting properties, Passive film, Mott–Schottky (M–S) analysis

## 1. INTRODUCTION

Stainless steel is the general name of some Fe-based alloys that have a high amount of Cr (more than 11 wt. %) and changing Ni amounts. There are three major kinds of microstructures in stainless steels, i.e., ferritic, martensitic and austenitic. These microstructures might be

www.SID.ir

Archive of SID

gained by a proper adjustment in the chemistry of steel. Stainless steels are able to be divided in a couple of groups: Cr–Ni and the Cr types, based on chemical composition [1–3]. From these three major microstructures, stainless steels are divided to six major categories (Fig. 1). The distinct categories of stainless steels have various properties [1,4,5]. Whereas, the Fe–Cr alloy produces the basis, modern stainless steels, in addition to chromium, also have a host of other alloying elements whose existence increases special properties. Molybdenum is added to increase the resistance against pitting and nickel to obtain austenite. For instance, completely austenitic stainless steels are non-magnetic, but their ferritic and martensitic counterparts have ferromagnetism [1,5].

In order to exclude reinforcement corrosion in really aggressive ambiences, the use of stainless steels (specifically austenitic stainless steels) is getting highly popular in a lot of civil constructions in industrial and marine ambiences [6,7]. Selecting austenitic stainless steels like AISI 304 and AISI 316 due to their great corrosion behavior in different corrosive environments is a factual challenge. Their acceptable mechanical properties and widespread usage are the reasons these alloys are chosen. Their great corrosion resistance in diverse aggressive ambiences is mostly because of the formed protective passive layer on their surface [8]. Thus, passivity is explained as a fairly inactive condition in which the metal shows a more noble behavior than that of thermodynamic conditions.

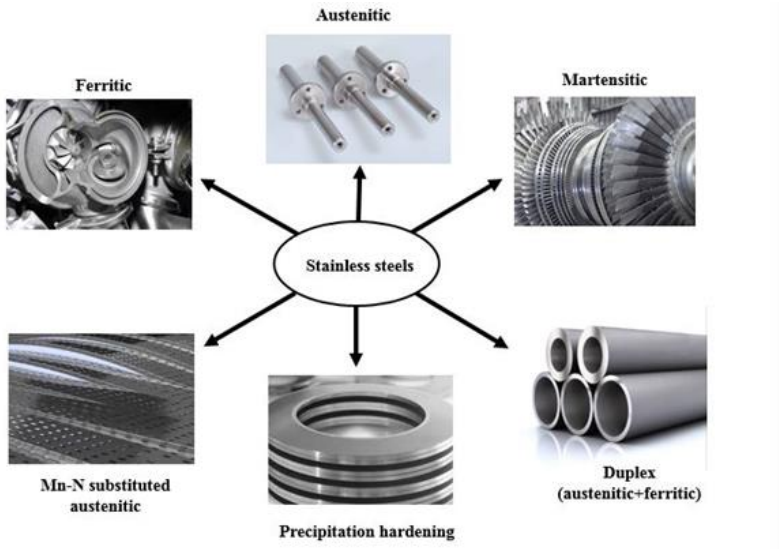


**Fig. 1.** Six major categories of stainless steels

## 2. PASSIVE FILM

Self-protection against corrosion of some metals is created by the passive layers growth in aqueous environments. This surface property is necessary to make sustainable developments in many usages and industries where metallic constituents are utilized. Passive layers do not mainly exceed a few nanometers of thickness at ambient temperature [9,10]. They are well

www.SID.ir

Archive of SID

adherent, hydroxylated and effectively separate the metals and alloys from the aggressive environment as well. However, passive layers are sensitive to local breakdown, in the existence of corrosive species, to accelerated dissolution for the substrate at limited sites [11,12]. The passive current density of many reactive transition metals (e.g., Ni, Fe, Cr) and their alloys that are faced with aqueous ambiences is of the order ~1.0−0.01 $\mu A/cm^2$ [13]. The very complicated passivation procedure can be influenced by several parameters like the composition of alloy, the formation conditions and the environment characteristics [8]. Oxide passive layers that were grown on surfaces of metal and alloy have been widely reviewed [11,14]. passive layers structure has been evaluated by atomic force microscopy and scanning tunneling microscopy for Fe, Cr, Ni and stainless steel [11].

Stainless steels are widely significant technological materials because of their widespread utility to form markedly $Cr^{3+}$-enriched passive films [8,11,12,15–17]. The Cr enrichment of the surface oxide formed in the passive range arises from a $Cr^{3+}$ small dissolution rate in comparison to $Fe^{2+}/Fe^{3+}$ oxides, having a diversity even more effective for chromium enrichment in acid aqueous ambiences [12]. Overpotential for passivation and ageing time have been revealed to clearly affect the crystallization of the passive layer atomic structure on ferritic (Fe-22Cr) and austenitic (Fe-18Cr-13Ni) single-crystal alloys [18–20], and on Fe-Cr [21,22] and AISI 304 [23] sputter-deposited layers, and simultaneously their dehydroxylation as measured by X-ray photoelectron spectroscopy (XPS) [18,19].

Realizing passivity and properties of passive film is a key element to protect stainless steels versus certain corrosion attack and one of the most current methods to decrease failures of localized corrosion-related requiring resistant materials selection by proper alloying [8,24–26]. The variations in stainless steels passive layer and its breakdown immediately affect the localized corrosion behavior resulting in crevice corrosion, pitting, stress corrosion cracking and intergranular attack. The properties of stainless steel passive layer can widely change considering the environment [27–29], film thickness, alloy composition, stoichiometry, structure, ionic conductivity, electronic band structure, etc. The stainless steels passive film is 1–3 nm thick depending on conditions of passivation [18,19,30–34].

The formed passive layer on stainless steels has been characterized composing of different bilayers. The inner film is enriched in Cr oxide whereas the outer film is a combination of Fe oxide and a hydroxide layer [8,35,36]. New investigations revealed that the formed passive layer on stainless steels composes of $Cr_2O_3$ and $Fe_2O_3$ as inner and outer films, respectively [8,28,29]. The bulk of $Cr_2O_3$ contains a hexagonal crystal structure [37]. New analysis by Rao et al. [38] has revealed that $Cr_2O_3$ can also make a cubic crystal structure. Thus, it is sensible to consider the oxide film has a constant volume composing of Cr and Fe oxides. The thickness of passive layer in a solution attains a steady-state because of being controlled by diffusion and the ions of oxygen with ions of cation reaction [39–43].

www.SID.ir

Archive of SID

## 3. MOTT–SCHOTTKY (M–S) ANALYSIS

In general, the passive layers are mostly composed of hydroxides or metallic oxides that are imagined as semiconductors. As a result, semiconducting behaviors are frequently seen on the surfaces of the passive metals and alloys. Their semiconducting behaviors are envisaged to be really significant for realizing the protective properties against corrosion. M–S analysis has been highly utilized in order to investigate the passive films semiconducting behaviors including the passive layers on Cr [44], Ni [45,46], Ni-base alloys [47–52], Zn [53], Cu [54–63], Al [64–67], Ti [68–77], Ti-6Al-4V [78], Ta [79–86], Mg alloys [87–93], W [85], Zr [94], and carbon steels [95–97].

In the recent years, increasing study of the semiconducting behaviors of stainless steels has given a significant help to the comprehension of these alloys corrosion resistance [98–107]. Based on the dominant imperfections in the passive layer either p- or n-type behaviors are seen. The passive layers having a lack in metal ions or extra cation vacancies have normally p-type behaviors. Likewise, n-type is made in the passive layers either by anion vacancies or extra cation in interstitial sites. M–S analysis has been indicated to be a significant in-situ technique to study passive films semiconductor properties. In order to measure the capacitance, the concept of electrochemical double layer (EDL) capacitance created in the passive layer near the interface of film–solution is normally created and the measured capacitance correlates with the space charge area that was created at this interface. When the oxide or passive layers are faced with a solution, the created space charge area and the Helmholtz film can be introduced as two condensators in series. Therefore, the measured capacitance for the interface of film–solution can be explained by the relation below [8]:

$$\frac{1}{C} = \frac{1}{C_{SC}} + \frac{1}{C_H} \tag{1}$$

where $C_{SC}$ and $C_H$ stand for the space charge and Helmholtz capacitance, respectively. Indicated as the M–S relation the expression turns into [8,47,108,109]:

$$\frac{1}{C^2} = \frac{1}{C_{SC}^2} + \frac{1}{C_H^2} + \frac{2}{C_{SC}C_H} \tag{2}$$

For Si and Ge (the classical semiconductors) described by a doping density about $10^{16}$ $cm^{-3}$, the $C_{SC}$ is really small in comparison to that of the $C_H$. In these status, the second and third terms contribution can be deleted. When the heavily doped ($10^{19}$–$10^{20}$ $cm^{-3}$) passive layers are pondered, the $C_{SC}$ area gets significant (but is still smaller than that of the $C_H$) [110]. In this case, the interface of passive layer–solution can be characterized using the relation that can be limited to the M–S relation [8]:

$$\frac{1}{C^2} = \frac{1}{C_{SC}^2} + \frac{1}{C_H^2} + \frac{2}{qN_q\varepsilon\varepsilon_0}\left(E - E_{FB} - \frac{kT}{e}\right) \tag{3}$$

www.SID.ir

Archive of SID

where *N*q is the densities of donor ($N_D$) or acceptor ($N_A$), $\varepsilon$ is the passive film dielectric constant, $\varepsilon_0$ stands for the vacuum permittivity, q stands for the elementary charge, *k* stands for the Boltzmann constant, and $U_{FB}$ shows the flat-band potential.

Based on the point defect model (PDM) [14,40–43], the defects in the passive layer are cation and oxygen vacancies, and cation interstitials. It is considered that vacancies of oxygen and cation interstitials are electron donors, leading to n-type doping when vacancies of cation are electron acceptors and as a result, doping the barrier film p-type. M–S measurement is a strong approach in order to measure the passive layers semiconductive properties on metals and their alloys [111–116]. This technique is according to the presence of a depletion area in the passive layer creating a $C_{SC}$. M–S relations that are utilized in order to specify the dopant density and semiconductor type of the passive layers, are [28,29,102,117]:

$$\frac{1}{C^2} = \frac{2}{\varepsilon\varepsilon_0 e N_D}\left(E - E_{FB} - \frac{kT}{e}\right) \qquad \text{n-type behavior} \tag{4}$$

$$\frac{1}{C^2} = -\frac{2}{\varepsilon\varepsilon_0 e N_A}\left(E - E_{FB} - \frac{kT}{e}\right) \qquad \text{p-type behavior} \tag{5}$$

It must be mentioned that the above relations are written considering that the EDL capacitance contribution is negligible [28,29,102,117].

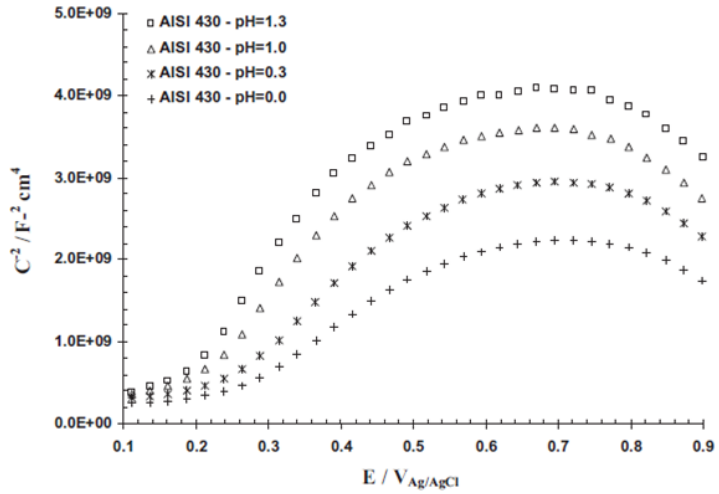


**Fig. 2.** M–S plots of AISI 430 stainless steel in $HNO_3$ solutions with pH varying from 1.3 to 0.0 [99]

## 4. SEMICONDUCTING PROPERTIES OF FERRITIC STAINLESS STEELS

Table 1 indicates the ferritic stainless steels semiconducting properties [118–127]. The pH of solution effect on the AISI 430 ferritic stainless steel (AISI 430) semiconducting properties within concentrated acidic electrolytes (pH varying from 0 to 1.3) [99] and concentrated alkaline solutions (pH varying from 11.5 to 14.0) [101] was investigated by Fattah-alhosseini

www.SID.ir

*Archive of SID*

and Vafaeian. In solutions of concentrated acidic, M–S test divulged that formed passive layers on AISI 430 treat p- and as n-type semiconductors and the $N_A$ and $N_D$ enhanced by declining pH (Fig. 2).

**Table 1.** The semiconducting properties of ferritic stainless steels

| **Ferritic stainless steel** | **Solution** | **Semiconducting behavior** | **Year** | **First author [Ref]** |
|---|---|---|---|---|
| ITM 40 | 1 N $H_2SO_4$, 1 N NaOH<br>1 N $H_2SO_4$ buffered to pH = 6.5 and 8.4 | $N_D$ in the range $10^{20}$-$10^{21}$ $cm^{-3}$ have been obtained at 1 kHz | 1989 | Di Palo [118] |
| AISI 434 | Hydrogen atmosphere | A fermi level pinning over a large potential region is deduced from M-S plots | 1990 | Gorse [119] |
| AISI 434 | Hydrogen atmosphere | A Fermi level pinning is observed over a large potential region | 1992 | Gorse [120] |
| Fe-17Cr , Fe-17Cr-5Mo<br>Fe-17Cr-10Mo | A buffer solution (pH 9.2)<br>0.05 M $H_3B0_3$ + 0.075 M $Na_2B_4O_7.10\ H_20$ | Addition of Mo decreases the $N_D$ of the deep level | 1996 | Hakiki [121] |
| AISI 409 | Simulated automotive exhaust gases at 400 °C | $SO_2$ may reduce the defects such as $Fe^{2+}$ ions in the thermal iron oxide layers | 2014 | Li [122] |
| AISI 430 | Highly concentrated LiBr solution | Passive films formed on stainless steels are made up of complex spinel oxides | 2014 | Fernández-Domene [123] |
| AISI 430 | Simulated concrete pore media | Passive film presenting a thinner n-type layer and its primary constituents of passive film is (Cr, Fe)-oxides | 2015 | Luo [124] |
| AISI 430 | Alkaline environment | Passive film presenting a thinner n-type layer in simulated concrete pore solution | 2015 | Luo [125] |
| AISI 430 | Concentrated acidic solutions<br>(pH varying from 0 to 1.3) | Passive film behaves as *n*-type and *p*-type semiconductors and the $N_D$ and $N_A$ increased with decreasing pH | 2015 | Fattah-alhosseini [99] |
| AISI 430 | Concentrated alkaline solutions<br>(pH varying from 11.5 to 14.0) | Passive films behave as n-type semiconductor and $N_D$ increased with pH | 2015 | Fattah-alhosseini [101] |
| Sn alloyed ferritic S.S | Simulated concrete solution in presence of NaCl | The p and n-type bilayer structure passive film were observed | 2018 | Luo [126] |
| Fe-20Cr | Sulfuric acid solution | Characteristic potential decay behavior is due to the duplex layer structure of passive film | 2018 | Kim [127] |

Fig. 2 indicates the M–S plots related to AISI 430 in solutions of $HNO_3$ having the pH that changes in a range from 1.3 to 0.0 [99]. It should be considered that for this alloy, $C^{-2}$ obviously declines by declining pH. Based on Fig. 2, the negative and positive slopes of the principal

*www.SID.ir*

Archive of SID

passive area are ascribed to behaviors of n- and p-type, respectively. Fig. 3 indicates the M–S plots of AISI 430 within NaOH solutions having pH that changes in a range from 11.5 to 14.0 [101]. It should be considered that $C^{-2}$ obviously declines by rising the pH for this alloy. According to Fig. 3, the positive slopes of the main passive area are ascribed to behavior of n-type.

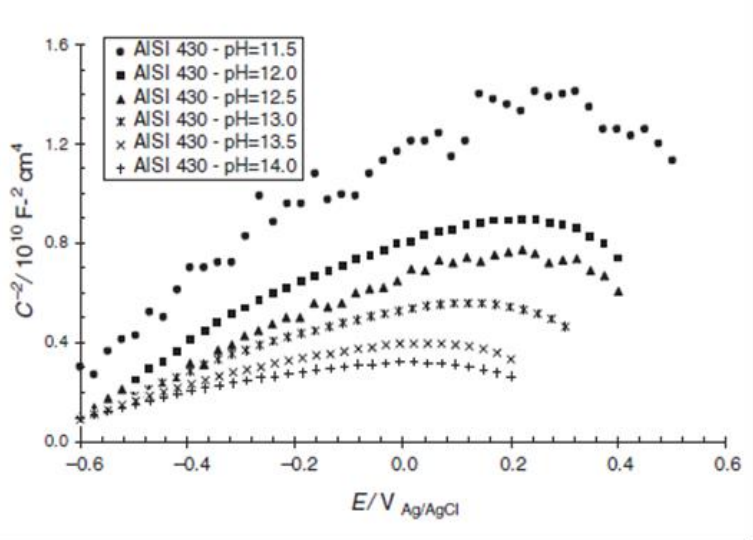


**Fig. 3.** M–S plots of AISI 430 stainless steel in NaOH solutions with pH varying from 11.5 to 14.0 [101]

## 5. INFLUENCE OF GRAIN REFINEMENT ON THE SEMICONDUCTING PROPERTIES

Stainless steels that have really higher corrosion resistance than those of other steel families, have drawn special attention in the field of grain refinement for producing alloys that have increased both mechanical and corrosion properties [128]. Among all stainless steels grades, austenitic ones have been noted as the subject of grain refinement for most of studies. The main reason of this specific attention is martensite procedure in which the strain-induced martensite reversion transformation (produced by heavy cold roll) to austenite (by annealing treatment) leads to a major grain refinement [128].

Responding the question regarding the effect of grain refinement on corrosion resistance is not easy. This subject is still investigated by some researchers [2,129,130]. Wu et al. [131] ascribed an enhancement in the corrosion of Fe–Ni–Cr alloy using grain refinement. But, the FG AISI 304 stainless steel corrosion resistance indicated more development comparing with coarse-grained (CG) steels within a solution of borate buffer having chloride and without it at two various temperatures [132]. The development in corrosion behavior of FG AISI 304 has been explained in solution of 0.5 M $H_2SO_4$ [133].

www.SID.ir

Archive of SID

The ferritic stainless steel has a grain refinement potential that is lower than that of austenitic grades due to the lack of martensite procedure. However, some investigations indicated that the mechanical properties of ferritic grades of stainless steels can be improved by decreasing the grain size [134,135]. Moreover, because of the rise in price of Ni, the requirements and usages of ferritic stainless steels are increasing nowadays and in some conditions the substitution of an austenitic steel by some low-cost ferritic stainless steels is possible [128]. Table 2 indicates how the grain refinement affects the semiconducting properties of ferritic stainless steels [100,102,103,106].

**Table 2.** The influence of grain refinement on the semiconducting properties of ferritic stainless steels

| **Ferritic stainless steel** | **Solution** | **Semiconducting behavior** | **Year** | **First author [Ref]** |
|---|---|---|---|---|
| AISI 430 | 0.1 M $HNO_3$ | Passive films behave as n-type and p-type semiconductors and grain refinement did not change the semiconductor type of the passive films. $N_D$ and $N_A$ decreased with grain refinement. | 2015 | Fattah-alhosseini [100] |
| AISI 430 | 0.1 M NaOH | Passive films behave as n-type and p-type semiconductors and the semiconductor character of the passive films did not change by grain refinement. $N_D$ and $N_A$ densities increased with grain refinement. | 2015 | Fattah-alhosseini [102] |
| AISI 430 | 0.1 M NaOH | Fine-grained (FG) sample showed higher $N_D$ and $N_A$ in comparison to coarse-grained (CG) one. | 2016 | Vafaeian [103] |
| AISI 430 | 0.1 M $HNO_3$ | Semiconducting behavior of FG sample in comparison with CG one was distinguished by its less charge carrier densities within the passive film. | 2017 | Vafaeian [106] |

Fig. 4 shows the schematic of advanced thermomechanical process used to obtain FG AISI 430 [103]. More details about this advanced thermomechanical procedure have been described [100,102,103,106,128]. Scanning electron microscope (SEM) micrographs of FG and CG AISI 430 specimens are indicated in Fig. 5 [102]. It is obvious that the advanced thermomechanical procedure considerably declined the grain size. Indeed, the grain size lessened about 100 times using the advanced thermomechanical procedure [102,103].

www.SID.ir

Archive of SID

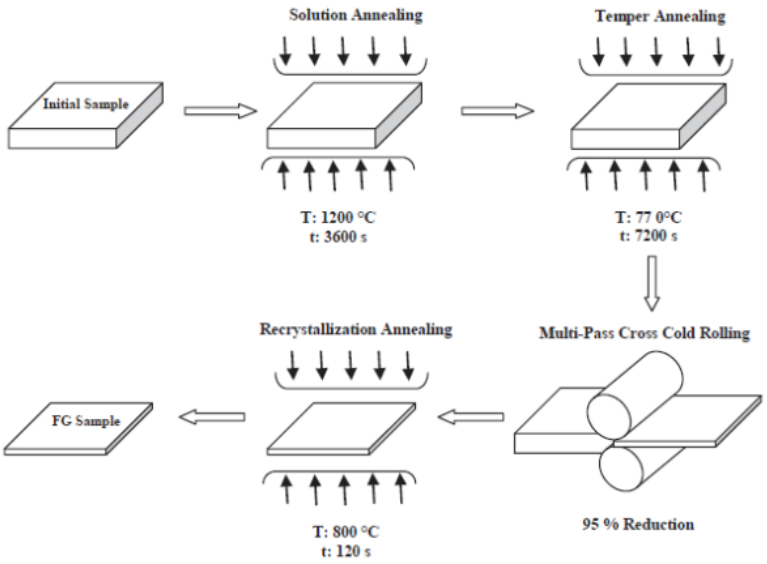


**Fig. 4.** Schematic illustration of advanced thermomechanical process used to obtain FG AISI 430 ferritic stainless steel [103]. (With permission from Ref. [103]; License Number: 4707710655144, License date: Nov 14, 2019)

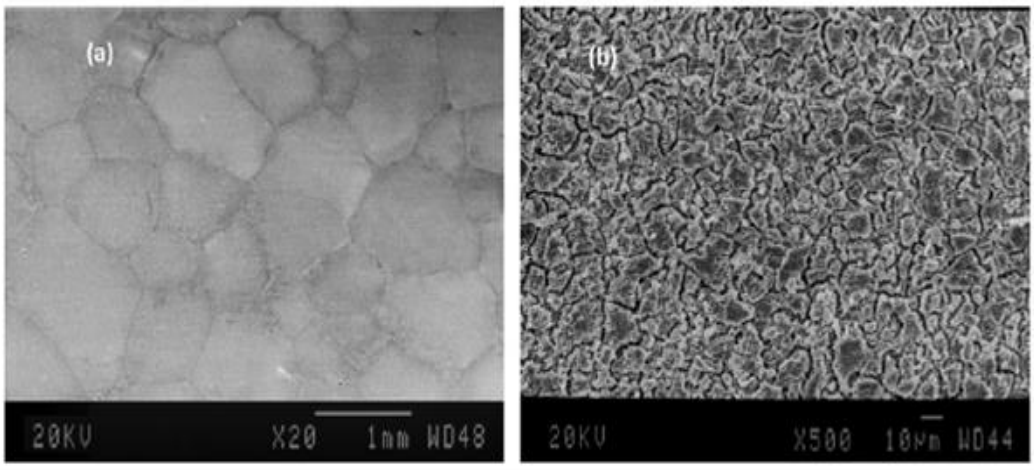


**Fig. 5.** SEM images of (a) CG and (b) FG AISI 430 ferritic stainless steel [102]. (With permission from Ref. [102]; License Number: 4707710316390, License date: Nov 14, 2019)

Fig. 6a indicates the plots of M–S for the passive layers that were produced on FG and CG specimens in solution of 0.1 M $HNO_3$. Based on Fig. 6a, both passive layers on FG and CG specimens showed duplex structure based on their p- and n-type behaviors. These properties are in a sensible agreement with the obtained results in former investigations for other stainless steels within acidic electrolytes [28,29]. In addition, both curves show the same properties and include three distinguished areas. The negative slopes in areas I and III are ascribed to p-type semiconducting behavior, whereas the positive slope in region II is attributed to the n-type semiconducting behavior [27,28]. The observed p-type behavior in area I is due to the existence

www.SID.ir

Archive of SID

of $Cr_2O_3$ in the inner part of the passive layer [136,137]. In area III, the p-type behavior can be corresponded to an increment in the passive layer conductivity because of the oxidation of $Cr^{3+}$ to $Cr^{6+}$. Furthermore, this behavior can be described via the production of cation vacancies (p-type dopants and electron acceptors) at the solution interface/passive layer [29,138].

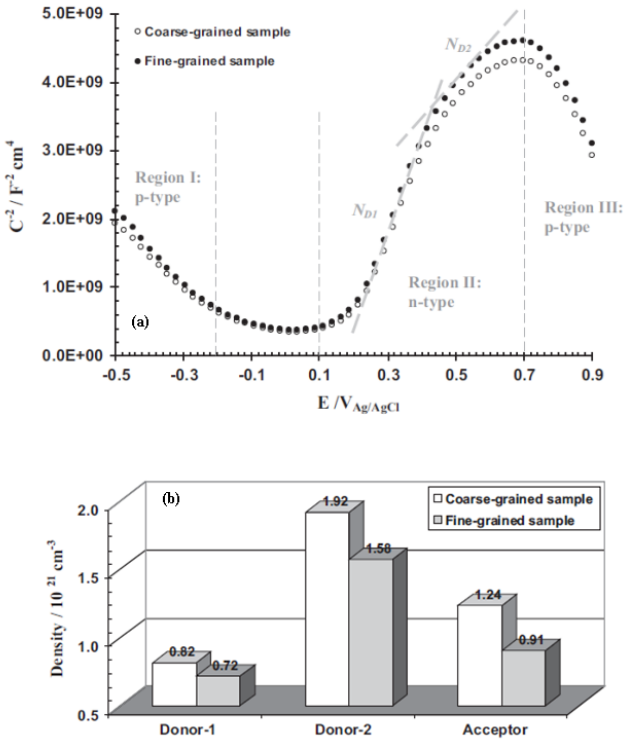


**Fig. 6.** (a) M–S plots and (b) variations in the $N_D$ and $N_A$ of CG and FG samples in 0.1 M $HNO_3$ solution [100]. (With permission from Ref. [100]; License Number: 4707701349217, License date: Nov 14, 2019)

It is realized that the M–S plots for bulk metal oxides such as $Fe_2O_3$ indicate no breakdown of linearity, and the behavior of n-type is ascribed to the existence of $Fe^{2+}$ cations [139]. The source of the two obtained slopes for produced passive layers on stainless steels in the anodic branch is still discussed [100]. Hakiki et al. [140] realized that the first and second slopes are ascribed to $Fe^{2+}$ located in the tetrahedral and octahedral. It was also proved these levels are related to oxygen vacancies and $Fe^{2+}$ in sites of octahedral. But, n-type properties were seen with passive layers that were produced on ferritic stainless steels despite their low amount of $Fe^{2+}$ [100].

Based on Eqs. (4) and (5), $N_D$ and $N_A$ have been obtained from the slopes of positive and negative. Fig. 6b indicates the $N_D$ and $N_A$ for the produced passive layers on FG and CG specimens in solution of 0.1 M $HNO_3$ [100]. The magnitude orders are about $10^{21}$ $cm^{-3}$ and are similar to those obtained for other stainless steels in acidic electrolytes [28,29]. Based on Fig.

www.SID.ir

*Archive of SID*

6b, $N_D$ and $N_A$ of the passive layer that were produced on the FG specimen were less than those of the CG specimen that reflected better passivation properties of the FG specimen. In other words, the amount of point defects was declined in the produced passive layer on the FG specimen whereas the CG specimen showed a very defective passive layer. These results showed that $N_A$ and $N_D$ were affected by the structure grain size and both of them are declined by grain refinement. Thus, passive layer is denser for FG rather than CG specimen in 0.1 M $HNO_3$ via the grain refinement [100].

Fig. 7a indicates the plots of M–S for the passive layers being produced on FG and CG specimens in solution of 0.1 M NaOH [102]. It is demonstrated that the M–S plots display positive and negative slopes that means the passive layers possess n- and p-type properties, respectively. The semiconductive behavior of p-type is ascribed to Cr-rich inner film, whereas the semiconductive behavior of n-type is ascribed to Fe-rich outer layer. The measured $N_D$ and $N_A$ of the produced passive layers on FG and CG specimens in solution of 0.1 M NaOH are exhibited in Fig. 7b. For both samples, the magnitude orders of carrier densities are about $10^{21}$ $cm^{-3}$, however, according to Fig. 7b, the $N_A$ and $N_D$ of the produced passive layer on the FG specimens are more than those of the CG ones. Thus, the amount of point defects in the produced passive layer on the FG specimen is augmented within alkaline solution. This leads to an improvement in electron transfer into the solution and loosing passivation resistance.

Based on the accomplished investigations about a passive layer atomic structure on stainless steels, it is indicated that this layer has a distinct structure in acidic ambiences comparing with alkaline/neutral electrolytes [29,141–143]. It is highly accepted that the produced passive layers on Fe–Cr alloys possess a bilayer structure, consisted of outer and inner layer whose composition changes by changing the pH of solution. The following instances shed more light on this matter. Haupt and Strehblow [144], studied the production of a passive film on alloys of Fe–Cr in 0.5 M $H_2SO_4$ from a surface analytical and electrochemical standpoint. Their measurements of ion scattering spectroscopy and XPS that were closely related to their electrochemical investigations indicated that the passivation of Fe–Cr in 0.5 M $H_2SO_4$ results in a pronounced increment of Cr in the passive layer due to a really small dissolution of Cr and the preferential dissolution of Fe. Carmezim et al. [145] assessed the electrochemical properties of AISI 304 and 446 within solutions having pH between 8.4 and 0.6. The acquired consequences of the produced passive film on both kinds of stainless steel can be explained by a duplex model, composing of an inner anhydrous film, rich in Cr oxides, and an outer hydrated film, enriched in Fe. In addition, it was depicted that while the pH of solution gets more acidic, the ratio of Cr to Fe in the layer enhanced remarkably. Schmutz and Landolt [146] measured the passivation properties of Fe-25Cr in both acidic and alkaline situations using some approaches like electrochemical quartz crystal microbalance (EQCM) to control the mass change and XPS test to analyze the passive layer chemical composition. In solution of 0.1 M $H_2SO_4$+0.4 M $Na_2SO_4$, an enhancement in the potential of Fe–25Cr in the

*www.SID.ir*

Archive of SID

passive zone resulted in a reduction because of preferential dissolution of Fe whereas, in 0.1 M NaOH, Fe–25Cr depicted a mass increase when the potential was enhanced. XPS studies indicated that in acidic solution, the passive layer got enriched in Cr oxide whereas, it had mainly Fe oxide in alkaline solution.

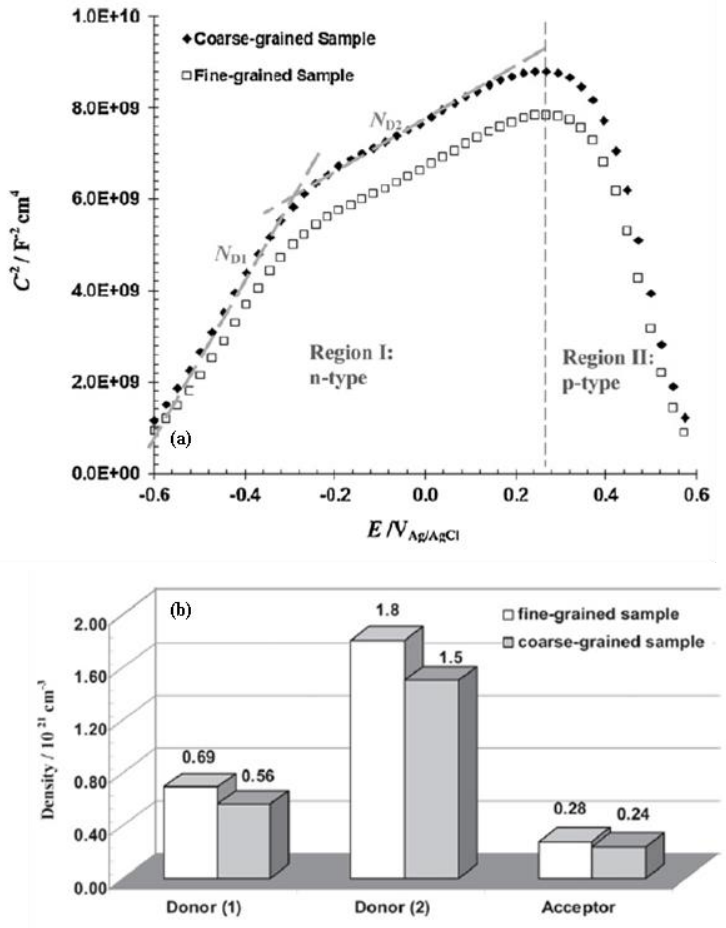


**Fig. 7.** (a) M–S plots and (b) variations in the $N_D$ and $N_A$ of CG and FG samples in 0.1 M NaOH solution [102]. (With permission from Ref. [102]; License Number: 4707710316390, License date: Nov 14, 2019)

Indeed, in an acidic ambience, the outer passive film is mainly enriched in Cr oxide/ hydroxide because of preferential dissolution of Fe whereas, in alkaline and neutral environments, the outer passive layer is mainly enriched in Fe oxide/ hydroxide due to preferential dissolution of Cr and more stability of Fe oxide in higher pH. It is worth implying that a lot of researchers have mentioned that FG stainless steels indicated better corrosion resistance and passivation properties in acidic electrolyte. The main cause is the FG structures surface got enriched quicker in Cr or reduced easier in Fe. On the other hand and based on our experiment, due to less stability of Cr oxides in comparison to Fe oxide, grain refinement makes quick depletion of Cr surface and so a weaker passive layer is produced in alkaline

www.SID.ir

Archive of SID

environment. In other words and according on the PDM, it can be mentioned that the less concentration of oxygen vacancy in the passive layer shows the higher protection of this layer [102]. Thus, in FG specimens and because of higher grain boundary density, the dissolution rate of Cr is really higher than those of CG ones. As a result, an enhancement in oxygen vacancy arising from such preferred dissolution makes the resistance of produced passive layer on FG specimens decline comparing with CG ones [102].

Fig. 8 shows the obtained M–S plots after employing distinct cycles by cyclic voltammetry (CV) measurement for FG and CG specimens in solution of 0.1 M NaOH, respectively [103]. As is clear in any of plots in Fig. 8, there are two areas having distinct slopes. Region (I) having positive slopes shows that the passive layer depicts n-type semiconductivity whereas region (II) having negative slope displays the passive layer divulges p-type semiconductivity. Thus, the plots of M–S for both FG and CG specimens having various cycles indicate same semiconducting behavior, however having various $N_D$ and $N_A$ as shown using distinct slopes of M–S curves [103].

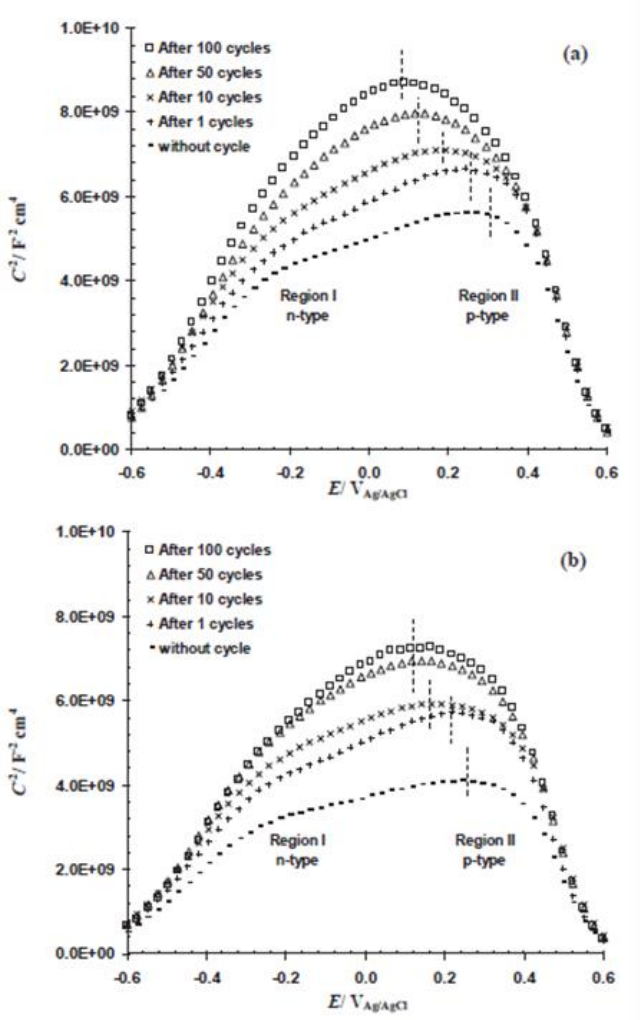


**Fig. 8.** M–S plots of (a) CG and (b) FG samples obtained after different numbers of cycles in 0.1 M NaOH solution [103]. (With permission from Ref. [103]; License Number: 4707710655144, License date: Nov 14, 2019)

www.SID.ir

Archive of SID

The $N_A$ and $N_D$ can be calculated according to the equations of M–S (Eq. (4) and (5)) and the negative and positive slopes of the M–S plots linear parts. The nonlinearity and appearance that is seen in the plots of M–S can be comparably seen in other investigations studying the semiconductive properties of stainless steels.

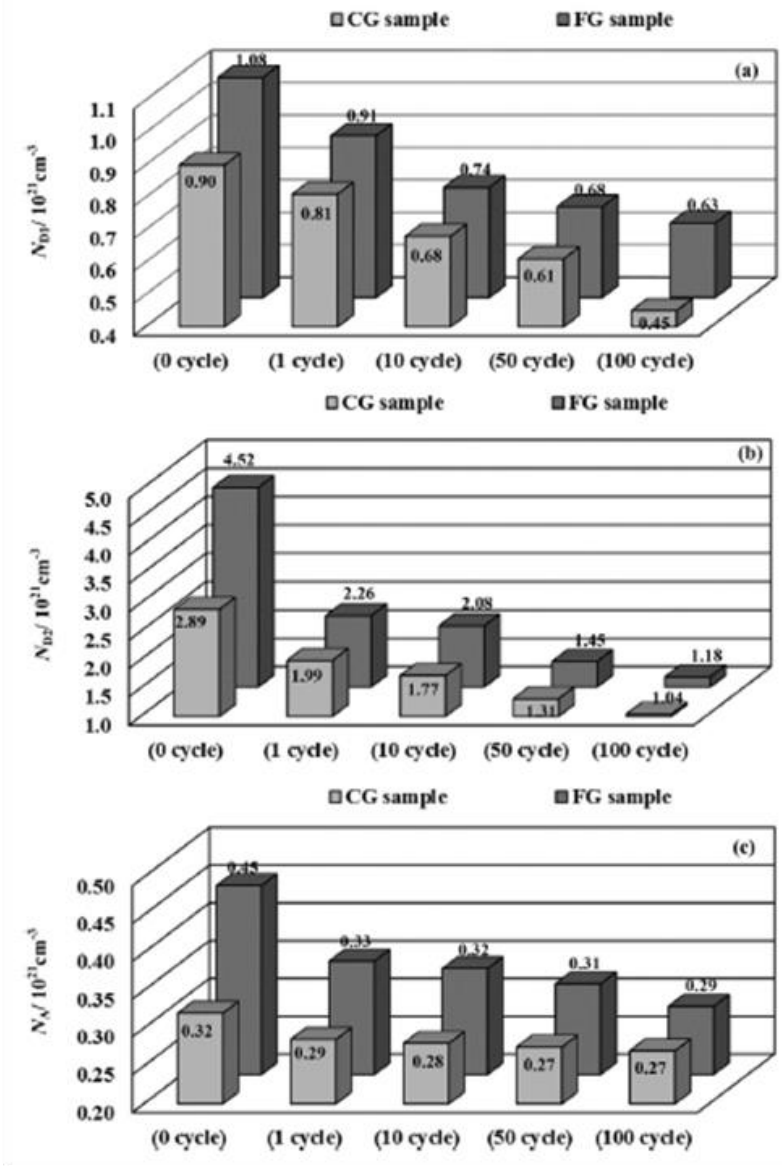


**Fig. 9.** Variations in the $N_D$ and $N_A$ of CG and FG samples in 0.1 M NaOH solution [103]. (With permission from Ref. [103]; License Number: 4707710655144, License date: Nov 14, 2019)

Various interpretations about the nonlinearity of M–S plots have been found by other researchers in the reticles like inhomogeneous donor distribution, the change in the potential of the Helmholtz layer, and dielectric relaxation of a disturbed surface film [147–149]. Fig. 9 shows the calculated $N_D$ and $N_A$ for both FG and CG specimens after employing distinct cycles, respectively [103]. In both FG and CG and specimens, the magnitude orders for charge carrier

www.SID.ir

Archive of SID

densities are about $10^{21}$ $cm^{-3}$. In addition, the $N_D$ and $N_A$ decline in both specimens by rising the number of cycles. Indeed, applying cyclic voltammetry passivation (CVP) is an effective approach in order to form less defective passive layer [103]. Differently, it can be seen that the charge carrier densities of FG specimen are higher than that of its CG one via comparing distinct graphs of Fig. 9.

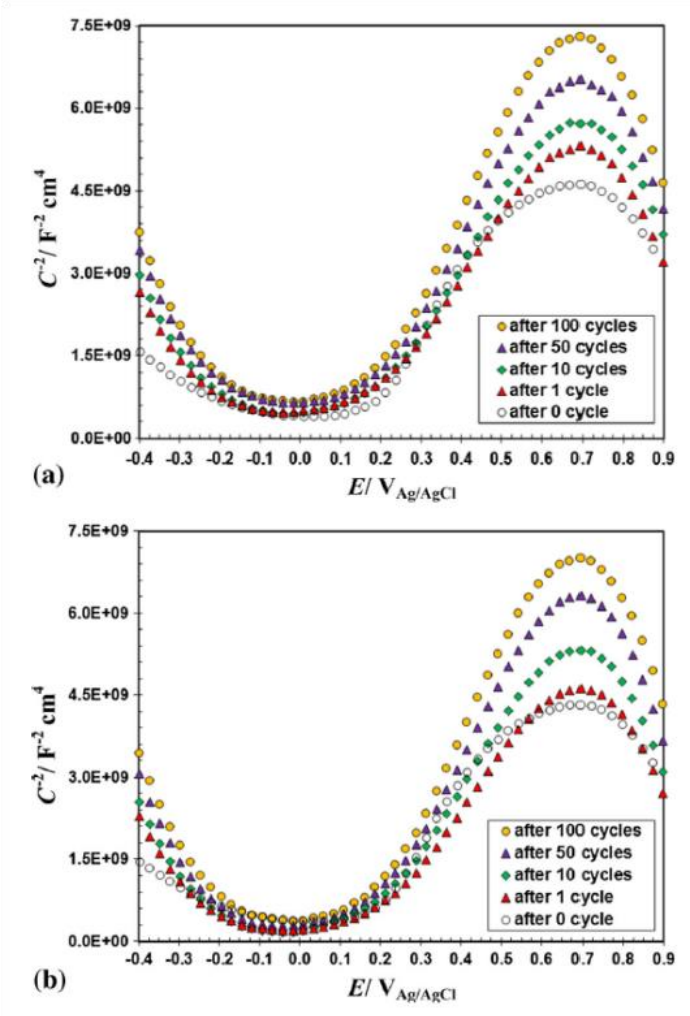


**Fig. 10.** M–S plots of (a) FG and (b) CG samples obtained after different numbers of cycles in 0.1 M $HNO_3$ solution [106]. (With permission from Ref. [106]; License Number: 4707721384331, License date: Nov 14, 2019)

Thus, the FG specimen weaker corrosion resistance comparing with CG one is maybe because of the existence of higher charge carrier densities in its passive layer that makes electron transfer easier into the solution. The FG specimen higher point defect density providing its dissolution easier [103,150].

The obtained M–S graphs of CG and FG specimens after employing various voltammetry cycles in solution of 0.1 M $HNO_3$ are indicated in Fig. 10 [106]. In each curve of Fig. 10, three regions having distinct slopes can be specified. The negative slopes in potential area (I) and

www.SID.ir

Archive of SID

(III) are ascribed to p-type properties whereas, positive slopes of potential area (II) are attributed to n-type properties. Both FG and CG specimens possess general semiconducting behavior due to the resemblance being in the forms of their M–S curves, however, the major difference is because of distinct slopes of M–S curves making a difference in $N_D$ and $N_A$ [106]. According to Eq. (4) and (5) and the slope of M–S line in Fig. 10, $N_A$ and $N_D$ and are measured. The calculation of $N_A$ and $N_D$ for both CG and FG samples after employing distinct voltammetry cycles is indicated in Fig. 11 [106].

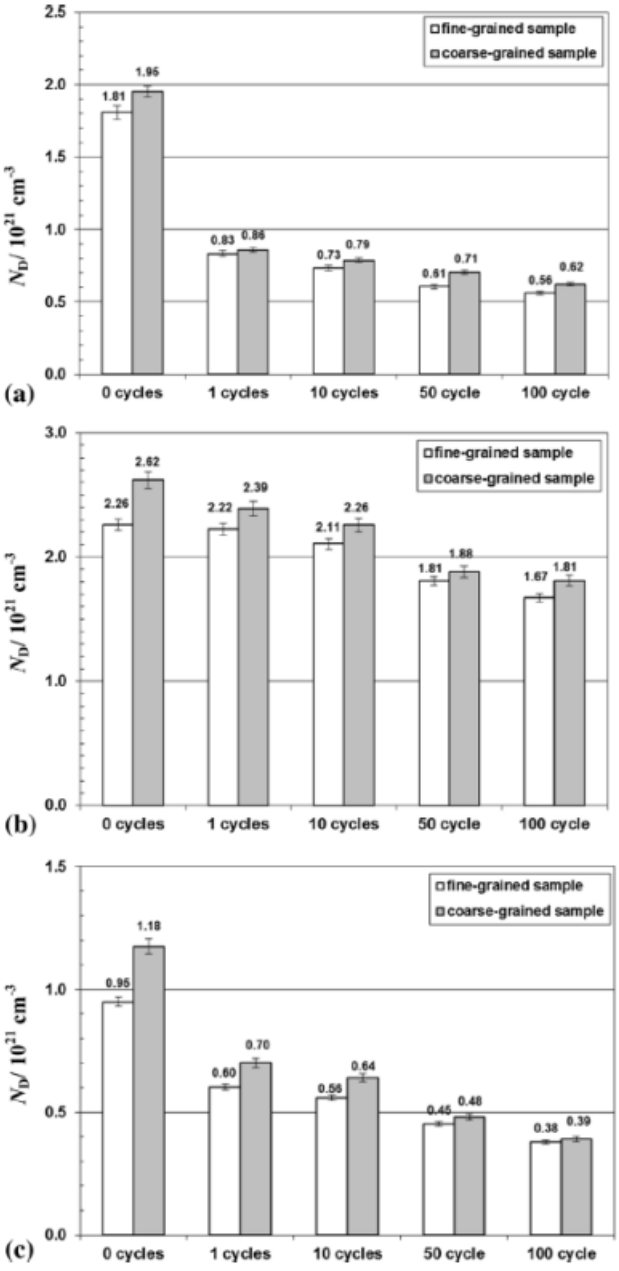


**Fig. 11.** Variations in the $N_D$ and $N_A$ of FG and CG samples in 0.1 M $HNO_3$ solution [106]. (With permission from Ref. [106]; License Number: 4707721384331, License date: Nov 14, 2019)

www.SID.ir

*Archive of SID*

The magnitude orders of charge carrier densities are about $10^{21}$ $cm^{-3}$ for both FG and CG and specimens. Furthermore, the charge carrier densities declined in both samples by rising the number of cycles. Indeed, employing CV resulted in a decline in some point defects in the passive layer. On the other hand, comparing distinct graphs of Fig. 11, indicates that the charge carrier densities in the passive layer of FG specimen are lower than that of CG specimen. Thus, the decrease in charge carrier densities was made by grain refinement caused electrons to transfer into the solution harder, that in turn leads to better corrosion resistance [106].

## 6. CONCLUSION

The effect of grain refinement on the semiconducting behavior of AISI 430 was studied by Mott–Schottky (M–S) test. M–S test depicted that the passive layers treat as p-type and n-type semiconductors and grain refinement did not vary the semiconductor behavior in solution of 0.1 M $HNO_3$. In addition, this test showed that the $N_A$ and $N_D$ was declined by grain refinement. M–S test indicated the passive layer on fine-grained (FG) specimens has higher point defect density in comparison to coarse-grained (CG) ones in solution of 0.1 M NaOH and thus less passivation resistance. The M–S test divulged that the passive layer of FG AISI 430 that was produced by CVP is more defective and thinner and indicates weaker corrosion resistance than that of its CG counterpart in solution of 0.1 M NaOH. Also, the M–S test indicated the produced passive layer on FG AISI 430 that was produced by CVP had less point defect density than that of CG one in solution of 0.1 M $HNO_3$ and thus, possessed higher passivation resistance.

## REFERENCES

[1] K. H. Lo, C. H. Shek, and J. K. L. Lai, Mater. Sci. Eng. R Reports. 65 (2009) 39.
[2] R. K. K. Gupta, and N. Birbilis, Corros. Sci. 92 (2015) 1.
[3] Q. Chen, and G. A. Thouas, Mater. Sci. Eng. R Reports. 87 (2015) 1.
[4] J. G. P. J. Beddoes, Introduction to Stainless Steels, ASM International (1999).
[5] M. Talha, C. K. Behera, and O. P. Sinha, Mater. Sci. Eng. C 33 (2013) 3563.
[6] A. Fattah-alhosseini, and H. Farahani, Iran. J. Mater. Sci. Eng. 10 (2013) 31.
[7] A. Fattah-alhosseini, and O. Imantalab, Iran. J. Mater. Sci. Eng. 11 (2014) 57.
[8] N. E. Hakiki, Corros. Sci. 53 (2011) 2688.
[9] A. Fattah-alhosseini, S. Taheri Shoja, B. Heydari Zebardast, and P. Mohamadian Samim, Int. J. Electrochem. 2011 (2011) 1.
[10] A. Fattah-Alhosseini, M. Mosavi,and A. Allahdadi, Int. J. Electrochem. 2011 (2011) 1.
[11] V. Maurice, and P. Marcus, Electrochim. Acta 84 (2012) 129.
[12] V. Maurice, and P. Marcus, Curr. Opin. Solid State Mater. Sci. 22 (2018) 156.
[13] A. Veluchamy, D. Sherwood, B. Emmanuel, and I. S. Cole, J. Electroanal. Chem. 785

*www.SID.ir*

Archive of SID

(2017) 196.
[14] D. D. Macdonald, Pure Appl. Chem. 71 (1999) 951.
[15] P. Marcus, Electrochim. Acta 43 (1998) 109.
[16] P. Marcus, and V. Maurice, Oxide Passive Films and Corrosion Protection, in: Oxide Ultrathin Film., Wiley-VCH Verlag GmbH & Co. KGaA, Weinheim, Germany (2012) pp. 119–144.
[17] H. H. Strehblow, Electrochim. Acta 212 (2016) 630.
[18] V. Maurice, J. Electrochem. Soc. 143 (1996) 1182.
[19] V. Maurice, J. Electrochem. Soc. 145 (1998) 909.
[20] T. Massoud, V. Maurice, L. H. Klein, and P. Marcus, J. Electrochem. Soc. 160 (2013) C232.
[21] M. P. Ryan, R. C. Newman, and G. E. Thompson, Philos. Mag. B 70 (1994) 241.
[22] M. P. Ryan, J. Electrochem. Soc. 141 (1994) L164.
[23] H. Nanjo, R. C. Newman, and N. Sanada, Appl. Surf. Sci. 121–122 (1997) 253.
[24] I. Olefjord, and L. Wegrelius, Corros. Sci. 38 (1996) 1203.
[25] C. O. Olsson, and D. Landolt, Electrochim. Acta 48 (2003) 1093.
[26] A. Fattah-alhosseini, A. Saatchi, M. A. Golozar, and K. Raeissi, J. Appl. Electrochem. 40 (2010) 457.
[27] A. Fattah-alhosseini, A. Saatchi, M. A. Golozar, and K. Raeissi, Electrochim. Acta 54 (2009) 3645.
[28] A. Fattah-alhosseini, M. A. Golozar, A. Saatchi, and K. Raeissi, Corros. Sci. 52 (2010) 205.
[29] A. Fattah-alhosseini, F. Soltani, F. Shirsalimi, B. Ezadi, and N. Attarzadeh, Corros. Sci. 53 (2011) 3186.
[30] V. Maurice, and P. Marcus, Prog. Mater. Sci. 95 (2018) 132.
[31] J. E. Castle, and J. H. Qiu, Corros. Sci. 29 (1989) 591.
[32] V. Maurice, H. Peng, L. H. Klein, A. Seyeux, S. Zanna, and P. Marcus, Faraday Discuss. 180 (2015) 151.
[33] R. Kirchheim, B. Heine, H. Fischmeister, S. Hofmann, H. Knote, and U. Stolz, Corros. Sci. 29 (1989) 899.
[34] P. Marcus, and I. Olefjord, Surf. Interface Anal. 11 (1988) 569.
[35] J. C. Colson, and J. P. Larpin, MRS Bull. 19 (1994) 23.
[36] D. D. Macdonald, J. Electrochem. Soc. 137 (1990) 2395.
[37] J. D. Hanawalt, and H. W. Rinn, Ind. Eng. Chem. Anal. Ed. 8 (1936) 244.
[38] J. C. Rao, X. X. Zhang, B. Qin, and K. K. Fung, Philos. Mag. Lett. 83 (2003) 395.
[39] C. Y. Chao, J. Electrochem. Soc. 128 (1981) 1187.
[40] D. D. MacDonald, Electrochim. Acta 56 (2011) 1761.
[41] Z. Lu, and D. D. Macdonald, Electrochim. Acta 53 (2008) 7696.

www.SID.ir

Archive of SID

[42] D. D. Macdonald, J. Electrochem. Soc. 153 (2006) B213.
[43] D. D. Macdonald, J. Nucl. Mater. 379 (2008) 24.
[44] D. S. Kong, S. H. Chen, C. Wang, and W. Yang, Corros. Sci. 45 (2003) 747.
[45] A. Fattah-alhosseini, M. Naseri, S. O. Gashti, S. Vafaeian, and M. K. Keshavarz, Corros. Sci. 131 (2018) 81.
[46] A. Fattah-alhosseini, M. Naseri, S. O. Gashti, S. Vafaeian, and M. K. Keshavarz, J. Mater. Eng. Perform. 27 (2018) 3401.
[47] A. Fattah-alhosseini, Z. Masomi, and M. Mirzaei, Anal. Bioanal. Electrochem. 6 (2014) 646.
[48] A. Fattah-alhosseini, Arab. J. Sci. Eng. 40 (2015) 63.
[49] A. Fattah-alhosseini, A. Jalali, and S. Felegari, Arab. J. Sci. Eng. 40 (2015) 2985.
[50] A. Fattah-alhosseini, H. Aghamohammadi, and A. B. Safa, Anal. Bioanal. Electrochem. 7 (2015) 728.
[51] A. Fattah-alhosseini, A. Khodabandeloie, and M. Bahiraee, J. Mater. Environ. Sci. 7 (2016) 1128.
[52] A. Fattah-alhosseini, N. Rohani, and F. Khodaei, Anal. Bioanal. Electrochem. 9 (2017) 174.
[53] A. Fattah-alhosseini, and M. Mirshekari, Trans. Indian Inst. Met. 68 (2015) 851.
[54] O. Imantalab, and A. Fattah-alhosseini, Anal. Bioanal. Electrochem. 7 (2015) 210.
[55] O. Imantalab, and A. Fattah-alhosseini, J. Mater. Eng. Perform. 24 (2015) 2579.
[56] A. Fattah-alhosseini, and O. Imantalab, J. Alloys Compd. 632 (2015) 48.
[57] A. Fattah-alhosseini, O. Imantalab, and F. R. Attarzadeh, J. Mater. Eng. Perform. 25 (2016) 4478.
[58] A. Fattah-alhosseini, O. Imantalab, and F. R. Attarzadeh, Metall. Mater. Trans. B 47 (2016) 2761.
[59] O. Imantalab, A. Fattah-alhosseini, Y. Mazaheri, and M. K. Keshavarz, Metall. Mater. Trans. A. 47 (2016) 3684.
[60] A. Fattah-alhosseini, and O. Imantalab, Metall. Mater. Trans. A 47 (2016) 572.
[61] D. Gholami, O. Imantalab, M. Naseri, S. Vafaeian, and A. Fattah-alhosseini, J. Alloy. Compd. 723 (2017) 856.
[62] A. Fattah-alhosseini, O. Imantalab, F.R. Attarzadeh, and N. Attarzadeh, J. Mater. Eng. Perform. 26 (2017) 1634.
[63] M. Naseri, D. Gholami, O. Imantalab, F. R. Attarzadeh, and A. Fattah-alhosseini, Mater. Res. Express. 5 (2018) 076504.
[64] S. O. Gashti, and A. Fattah-alhosseini, Anal. Bioanal. Electrochem. 6 (2014) 535.
[65] S. O. Gashti, A. Fattah-alhosseini, and Y. Mazaheri, Acta Metall. Sin. (English Lett. 29 (2016) 629.
[66] S. O. Gashti, A. Fattah-alhosseini, Y. Mazaheri, and M. K. Keshavarz, J. Manuf. Process.

www.SID.ir

Archive of SID

22 (2016) 269.
[67] S. O. Gashti, A. Fattah-alhosseini, Y. Mazaheri, and M. K. Keshavarz, J. Alloy. Compd. 688 (2016) 44.
[68] A. Fattah-alhosseini, F. R. Attarzadeh, and M. Vakili-Azghandi, Metall. Mater. Trans. A 48 (2017) 403.
[69] A. Fattah-alhosseini, M. Vakili-Azghandi, and M. Haghshenas, Int. J. Adv. Manuf. Technol. 90 (2017) 991.
[70] G. Ansari, and A. Fattah-alhosseini, Mater. Sci. Eng. C 75 (2017) 64.
[71] A. Fattah-alhosseini, A. R. Ansari, Y. Mazaheri, and M. K. Keshavarz, Mater. Sci. Eng. C 71 (2017) 771.
[72] A. Fattah-alhosseini, H. Elmkhah, and F. R. Attarzadeh, J. Mater. Eng. Perform. 26 (2017) 1792.
[73] F. R. Attarzadeh, H. Elmkhah, and A. Fattah-alhosseini, Metall. Mater. Trans. B 48 (2017) 227.
[74] A. Fattah-alhosseini, M. Vakili-Azghandi, M. Sheikhi, and M. K. Keshavarz, J. Alloy. Compd. 704 (2017) 499.
[75] A. Ebrahimi, H. Esfahani, A. Fattah-alhosseini, and O. Imantalab, J. Alloy. Compd. 765 (2018) 826.
[76] A. Ebrahimi, H. Esfahani, A. Fattah-alhosseini, and O. Imantalab, J. Mater. Eng. Perform. 28 (2019) 1456.
[77] A. Fattah-alhosseini, O. Imantalab, and G. Ansari, Mater. Sci. Eng. C 71 (2017) 827.
[78] A. Fattah-alhosseini, and S. Tofangsaz, Anal. Bioanal. Electrochem. 10 (2018) 414.
[79] A. Fattah-alhosseini, and S. Sharifi, Anal. Bioanal. Electrochem. 9 (2017) 862.
[80] F. R. Attarzadeh, N. Attarzadeh, S. Vafaeian, and A. Fattah-alhosseini, J. Mater. Eng. Perform. 25 (2016) 4199.
[81] A. Fattah-alhosseini, F. R. Attarzadeh, S. Vafaeian, M. Haghshenas, and M. K. Keshavarz, Int. J. Refract. Met. Hard. Mater. 64 (2017) 168.
[82] A. Fattah-alhosseini, and M. Pourmahmoud, J. Mater. Eng. Perform. 27 (2018) 116.
[83] A. Fattah-alhosseini, H. Elmkhah, G. Ansari, F. Attarzadeh, and O. Imantalab, J. Alloys Compd. 739 (2018) 918.
[84] A. Fattah-alhosseini, H. Elmkhah, K. Babaei, O. Imantalab, H. R. Ghomi, and M. K. Keshavarz, Mater. Res. Express. 5 (2018) 106401.
[85] A. Fattah-alhosseini, M. Roknian, and K. Babaei, Mater. Res. Express. 5 (2018) 116514.
[86] A. Fattah-alhosseini, S. Vafaeian, A. R. Ansari, and M. Khanmohammadi, Anal. Bioanal. Electrochem. 9 (2017) 660.
[87] A. Fattah-alhosseini, and M. Sabaghi Joni, J. Magnes. Alloy. 2 (2014) 175.
[88] A. Fattah-alhosseini, and M. Sabaghi Joni, J. Magnes. Alloy. 2 (2014) 305.
[89] A. Fattah-alhosseini, and M.S. Joni, J. Alloys Compd. 646 (2015) 685.

www.SID.ir

*Archive of SID*

[90] A. Fattah-alhosseini, and M. S. Joni, Int. J. Mater. Res. 106 (2015) 282.
[91] M. Sabaghi Joni, A. Fattah-alhosseini, and M. Javidi, Anal. Bioanal. Electrochem. 11 (2019) 448.
[92] A. Fattah-alhosseini, and H. Asgari, Arab. J. Sci. Eng. 41 (2016) 169.
[93] A. Fattah-alhosseini, and H. Asgari, J. Mater. Eng. Perform. 27 (2018) 3248.
[94] A. Fattah-alhosseini, and N. Attarzadeh, Anal. Bioanal. Electrochem. 7 (2015) 254.
[95] P. Mohamadian Samim, and A. Fattah-alhosseini, Anal. Bioanal. Electrochem. 8 (2016) 644.
[96] G. A. Zhang, and Y. F. Cheng, Electrochim. Acta 55 (2009) 316.
[97] D. G. Li, Y. R. Feng, Z. Q. Bai, J. W. Zhu, and M. S. Zheng, Appl. Surf. Sci. 254 (2008) 2837.
[98] S. Ningshen, U. Kamachi Mudali, V. K. Mittal, and H. S. Khatak, Corros. Sci. 49 (2007) 481.
[99] A. Fattah-alhosseini, and S. Vafaeian, Egypt. J. Pet. 24 (2015) 333.
[100] A. Fattah-alhosseini, and S. Vafaeian, J. Alloys Compd. 639 (2015) 301.
[101] A. Fattah-alhosseini, and S. Vafaeian, J. Mater. Res. Technol. 4 (2015) 423.
[102] A. Fattah-alhosseini, and S. Vafaeian, Appl. Surf. Sci. 360 (2016) 921.
[103] S. Vafaeian, A. Fattah-alhosseini, M. K. Keshavarz, and Y. Mazaheri, J. Alloy. Compd. 677 (2016) 42.
[104] P. Mohamadian Samim, and A. Fattah-alhosseini, Anal. Bioanal. Electrochem. 8 (2016) 717.
[105] A. Fattah-alhosseini, Arab. J. Chem. 9 (2016) S1342.
[106] S. Vafaeian, A. Fattah-alhosseini, M. K. Keshavarz, and Y. Mazaheri, J. Mater. Eng. Perform. 26 (2017) 676.
[107] F. Qods, S. Maryanaji, and A. Fattah-alhosseini, Anal. Bioanal. Electrochem. 10 (2018) 161.
[108] A. Fattah-alhosseini, and M. Asadi Asadabad, Iran. J. Mater. Sci. Eng. 11 (2014) 20.
[109] A. Fattah-alhosseini, A. Moradi, E. Moradi, and N. Attarzadeh, Anal. Bioanal. Electrochem. 6 (2014) 284.
[110] A. Fattah-alhosseini, F. Shirsalimi, M. Yousefi, and A. Abedi, J. Mater. Environ. Sci. 5 (2014) 1847.
[111] O. Imantalab, A. Fattah-alhosseini, M. K. Keshavarz, and Y. Mazaheri, J. Mater. Eng. Perform. 25 (2016) 697.
[112] A. Fattah-alhosseini, A. H. Taheri, and M. K. Keshavarz, Trans. Indian Inst. Met. 69 (2016) 1423.
[113] A. Fattah-alhosseini, M. Naseri, O. Imantalab, D. Gholami, and M. Haghshenas, J. Mater. Eng. Perform. 25 (2016) 4741.
[114] A. Fattah-alhosseini, and O. Imantalab, Anal. Bioanal. Electrochem. 8 (2016) 862.

*www.SID.ir*

*Archive of SID*

[115] A. Fattah-alhosseini, A. R. Ansari, Y. Mazaheri, and M. Karimi, J. Mater. Eng. Perform. 26 (2017) 611.
[116] R. Khatami, A. Fattah-alhosseini, and M. K. Keshavarz, J. Alloy. Compd. 708 (2017) 316.
[117] M. K. Keshavarz, and A. Fattah-alhosseini, Arab. J. Chem. (2018). doi:10.1016/j.arabjc.2018.01.021.
[118] A. Di Paola, Electrochim. Acta 34 (1989) 203.
[119] D. Gorse, B. Rondot, and B. Baroux, Corros. Sci. 31 (1990) 591.
[120] D. Gorse, J. C. Joud, and B. Baroux, Corros. Sci. 33 (1992) 1455.
[121] N. E. Hakiki, J. Electrochem. Soc. 143 (1996) 3088.
[122] M. C. Li, H. Zhang, R. F. Huang, S. D. Wang, and H. Y. Bi, Corros. Sci. 80 (2014) 96.
[123] R. M. Fernández-Domene, E. Blasco-Tamarit, D. M. García-García, and J. García-Antón, Thin Solid Films. 558 (2014) 252.
[124] H. Luo, H. Su, C. Dong, K. Xiao, and X. Li, Data Br. 5 (2015) 171.
[125] H. Luo, H. Su, C. Dong, K. Xiao, and X. Li, Constr. Build. Mater. 96 (2015) 502.
[126] H. Luo, H. Su, B. Li, and G. Ying, Appl. Surf. Sci. 439 (2018) 232.
[127] Y. Kim, S. Oh, S. Ahn, K. Oh, K. Jung, and H. Kwon, Electrochim. Acta 266 (2018) 1.
[128] S. Vafaeian, A. Fattah-alhosseini, Y. Mazaheri, and M. K. K. Keshavarz, Mater. Sci. Eng. A. 669 (2016) 480.
[129] K. D. Ralston, and N. Birbilis, Corrosion 66 (2010) 075005-075005–13.
[130] L. Liu, Y. Li, and F. Wang, J. Mater. Sci. Technol. 26 (2010) 1.
[131] Z. Wu, J. Chen, N. Piao, C. Sun, W. Hassan, X. Zhang, and Y. Xie, Trans. Nonferrous Met. Soc. China. 24 (2014) 1989.
[132] L. Jinlong, and L. Hongyun, J. Mater. Eng. Perform. 23 (2014) 4223.
[133] Z. J. Zheng, Y. Gao, Y. Gui, and M. Zhu, Corros. Sci. 54 (2012) 60.
[134] J. E. Jin, Y. S. Jung, and Y. K. Lee, Mater. Sci. Eng. A 449–451 (2007) 786.
[135] M. Rifai, H. Miyamoto, and H. Fujiwara, Ser. Mater. Sci. Eng. 63 (2014) 012122.
[136] N. B. Hakiki, S. Boudin, B. Rondot, and M. Da Cunha Belo, Corros. Sci. 37 (1995) 1809.
[137] S. Virtanen, J. Electrochem. Soc. 142 (1995) 3067.
[138] T. L. S. L. Wijesinghe, and D. J. Blackwood, J. Electrochem. Soc. 154 (2007) C16.
[139] P. Schmuki, J. Electrochem. Soc. 142 (1995) 3336.
[140] N. E. Hakiki, J. Electrochem. Soc. 145 (1998) 3821.
[141] W. Fredriksson, S. Malmgren, T. Gustafsson, M. Gorgoi, and K. Edström, Appl. Surf. Sci. 258 (2012) 5790.
[142] C. M. Abreu, M. J. Cristóbal, R. Losada, X. R. Nóvoa, G. Pena, and M. C. Pérez, Electrochim. Acta 51 (2006) 2991.
[143] T. Shibata, Critical Factors for Controlling the Stability of the Passive Film on Stainless Steels, in: ECS Trans., ECS, (2009) pp. 331–343.

*www.SID.ir*

Archive of SID

[144] S. Haupt, and H. H. Strehblow, Corros. Sci. 37 (1995) 43.
[145] M. J. Carmezim, A. M. Simões, M. F. Montemor, and M. Da Cunha Belo, Corros. Sci. 47 (2005) 581.
[146] P. Schmutz, and D. Landolt, Corros. Sci. 41 (1999) 2143.
[147] L. V. Jin-long, and L. Hong-yun, Mater. Chem. Phys. 135 (2012) 973.
[148] N. E. Hakiki, M. F. Montemor, M. G. S. Ferreira, and M. da Cunha Belo, Corros. Sci. 42 (2000) 687.
[149] A. M. P. Simões, J. Electrochem. Soc. 137 (1990) 82.
[150] A. Fattah-alhosseini, Gh. Ansari, and O. Imantalab, Anal. Bioanal. Electrochem.10 (2018) 805.

*Copyright © 2019 by CEE (Center of Excellence in Electrochemistry)*
**ANALYTICAL & BIOANALYTICAL ELECTROCHEMISTRY (**http://www.abechem.com**)**
*Reproduction is permitted for noncommercial purposes.*

www.SID.ir